

## Cosmic ray measurements inside ISS with Sileye3/Alteino experiment

M. Casolino<sup>a</sup> for the Sileye-3 collaboration

(a) INFN Rome 2 and University of Rome Tor Vergata, Dep. of Physics, Via della ricerca scientifica 1 00133 Roma, Italy  
 Presenter: M. Casolino (casolino@roma2.infn.it), ita-casolino-M-abs3-sh35-poster

We report on the measurements performed on board the International Space Station with the Sileye-3/Alteino experiment between 27/4 and 1/5/2002. The instrument is constituted of a cosmic ray silicon detector and an electroencephalograph to monitor radiation environment and study the light flash phenomenon in space. In this work we describe the relative nuclear abundance measurements in different regions of the orbit for nuclei from B to Fe in the energy range above  $\simeq 60$  MeV/n. As a result of nuclear fragmentation with the hull of the station, abundances of heavy nuclei (Fe group) are found to be reduced whereas lighter elements such as F and N are enhanced.

### 1. Introduction

The Sileye-3/Alteino experiment is devoted to the investigation of the Light Flash phenomenon and the study of cosmic ray particle flux and composition inside the ISS. This experiment follows previous ones on Mir where relative nuclear abundances and Light Flash perception [1, 2, 3] measurements have been performed. All nuclei are present in cosmic rays, with Helium as the most abundant component ( $\simeq 10\%$ ) after Hydrogen ( $\simeq 90\%$ ) resulting in a radiation field much different (both in intensity and composition) than what is encountered on Earth. Indeed, although much less abundant than protons, heavier nuclei represent the dominant component of the equivalent dose [4]. For the determination of the equivalent dose absorbed by astronauts and the validation of Montecarlo transport codes, it is of crucial importance to have a detailed measurement of the temporal and orbit dependent particle rate and composition. To this purpose a number of detectors have been operating on board spacecraft Mir, on the Shuttle, and are present on ISS [5, 7, 8, 9, 10, 6, 11, 12] to have a detailed picture of the particle fluence in space. Equally important is the accurate estimation of the damage to cells and the associated risk induced by heavily charged radiation on astronauts [13, 14, 15]. Alteino has a complementary nature to other devices as it is particularly suited to single and multiple cosmic rays detection and identification: in this work we present relative nuclear abundances from B to Fe measured inside ISS.

### 2. Nuclear abundances

Sileye-3 is a cosmic ray detector composed of 8 silicon strip detector planes, each divided in 32 strips, with 2.5 mm pitch., each  $380\mu\text{m}$  thick. There are 4 planes oriented along the X view and 4 planes along the Y view. Two scintillators (1 mm thick each) are located on top and bottom of the silicon stack to provide the trigger. Detector characteristics are described in [16, 17, 18].

To measure relative nuclear abundances inside Pirs (Russian airlock) module we have selected single tracks crossing the eight planes of the detector. The energy lost  $E_{loss}$  in silicon has been normalized to vertical incidence  $E_{loss\ norm.}$  according to the formula:  $E_{loss\ norm.} = E_{loss} \cos(\theta_{inc})$ , with  $\theta_{inc}$  the angle of incidence from the normal of the silicon planes. An additional cut, requiring that the energy released in the first and the last planes does not differ by more than 20% and selects particles of energy  $E_{kin} \gtrsim 60\text{ MeV/n}^1$ . At these energies the energy lost in the silicon, is small if compared to the kinetic energy of the particles. The average

<sup>1</sup>The energy loss of nuclei in matter is described by the Bethe Block formula and mostly depends from  $Z^2/\beta^2$ , with  $\beta = v/c$  and  $v$  the velocity of the impinging particle. The value of  $\beta$  of most cosmic rays selected with the above mentioned cut is close to 1, with

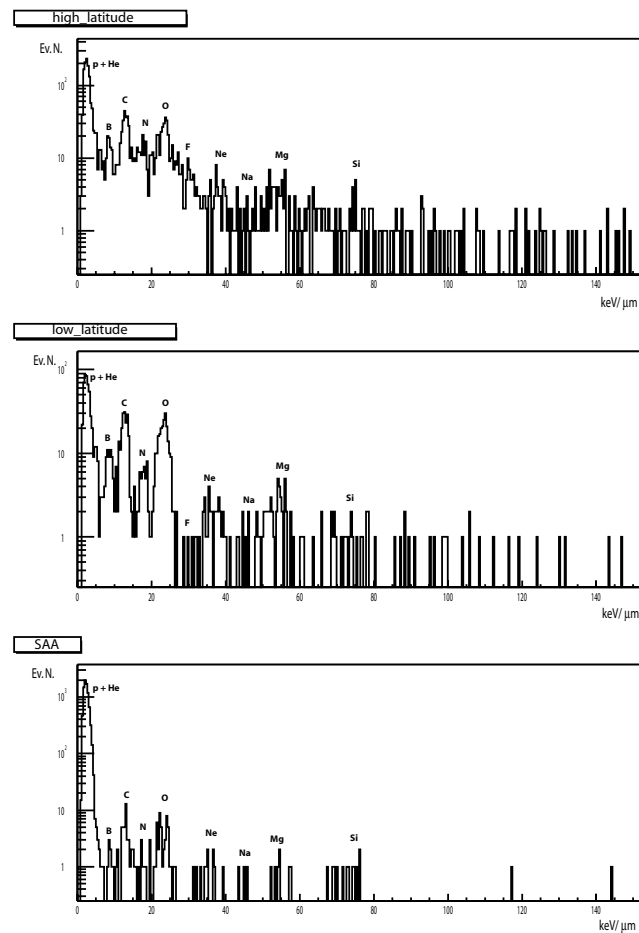


**Figure 1.** Elemental distributions measured in different regions of the orbit. Top: High latitude ( $L > 2$ ) region, Center: Low latitude region  $L < 2$ , Bottom: SAA. Note the higher abundance of protons (leftmost peaks) in the SAA and the sharper peaks in the low latitude region due to higher energy of the particles (rigidity cutoff  $G > 3.875$  GV) which is reflected in a smaller variation in the energy loss.)

energy loss in the silicon planes is thus constant and proportional to  $Z^2$  (the square of the electric charge). The particle spectrum resulting from these cuts is shown in Figure 2. The leftmost and highest peak is due to protons and helium, composing more than 95% of radiation in cosmic rays. It is possible to clearly distinguish the peaks from B to Si, with the odd number nuclei more abundant than even number, as in cosmic rays. The dynamic range of the electronics allows for nuclear detection up to As ( $Z=33$ ), although in this dataset Ca and Fe groups are limited by statistics. Trigger efficiency and silicon detector response for protons is currently being evaluated with Montecarlo simulations. It is possible to see that nuclear identification is possible with this analysis method for nuclei with  $Z \geq 5$ . To evaluate the relative nuclear abundances for these species we

---

only the less abundant component of low energy particles resulting in a higher energy release tail (For instance, 84% of Carbon nuclei in cosmic rays have  $1/\beta^2 < 1.2$ ).

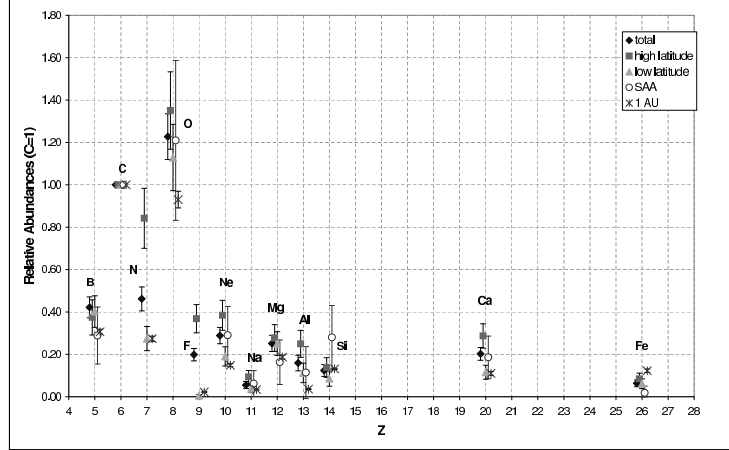


**Figure 2.** Relative Nuclear abundances (normalized to C=1) measured with Sileye-3 for the whole orbit and the three regions (see text). 1 AU data are taken from [19]. It is possible to see the O and Ca group enhancement. On the other hand the Fe group  $23 \leq Z$  is suppressed by a factor 2.

used a multigaussian fit of the form:

$$f(E) = \sum_i A_i * \exp\left(\frac{-(E-x_i)^2}{(2\sigma_i)^2}\right) \quad N_i = A_i * \sigma_i * \sqrt{(2\pi)} \quad (1)$$

Where  $N_i$  is the number of events of species  $i$ ,  $E$  is the energy released in the detector,  $x_i$  and  $\sigma_i$  are the mean value and sigma for species  $i$  and  $A_i$  is the normalization factor. The fit was performed using Minuit (in the ROOT framework) in groups of 4 nuclear species each for a total of 12 parameters ( $A_i$ ,  $x_i$  and  $\sigma_i$  for each species  $i$ ). This was done separately for the BCNO and FNeNaMg group: in the former case contamination from  $Z < 5$  elements was estimated with an exponential tail added to the fitting formula, whereas contamination of O over F was estimated by adding the O distribution to the fitting function. Higher  $Z$  elements do not have enough events to use this method. It was thus necessary to count the events in the expected energy range for each nuclear group (Al, Si, Ca, Fe). Peak position was determined assuming a linear response in the detector; the  $\sigma$  was scaled accordingly. From this it was possible to estimate relative contamination between groups and the resulting statistical error. In this analysis we have considered only data from two memory cards, since in the first one some events are saved incorrectly. This should not result in a wrong *relative* abundance measurement but we are currently considering in detail this phenomenon and we will include these data in a next analysis. The active nature of the detector allows us to study effects dependent on geographic regions. We have divided the orbit of the space station in three regions: a) *A high latitude region* (time of permanence 29%) (McIlwain parameter  $L > 2$ ), where the cutoff in rigidity  $G$  is lower and particle flux is higher; b) *The South Atlantic Anomaly* (SAA - time of permanence 13%) (geomagnetic field  $B < .25G$ ) c) *The remaining low latitude* ( $L < 2$ ) and high cutoff ( $G > 3.9GV$ ) region (time of permanence 58%). The resulting plots are shown in Figure 1: Event though they are not normalized by the time spent in each region, it is possible to see the higher counts in the  $L > 2$  region (due to the lower cutoff) and the trapped protons in the SAA (more than one order of magnitude more abundant than in other regions)

Relative abundances - normalized to carbon - are shown in Figure 2 for the whole orbit and the three regions

and compared with data outside the station [19]. It is possible to see how oxygen is more abundant than carbon in all regions; furthermore odd numbered nuclei such as nitrogen and fluorine are enhanced (respectively by a factor 2 and 10) by nuclear fragmentation inside the station. This effect is more evident on these low abundance nuclei. This phenomenon is more evident at high latitudes, where the low energy particles are more abundant and have a higher fragmentation cross section. It is also possible to see how the Ca group ( $15 \leq Z < 23$ ) and Fe group ( $23 \leq Z$ ) are respectively enhanced and suppressed by a factor 2 in their interaction with the station.

## References

- [1] Avdeev S., Bidoli V., Casolino M. et al, Eye light flashes on the Mir space station, *Acta Astronautica*, 50(8), 511-25 (2002)
- [2] Bidoli V., Casolino M., De Grandis E. et. al, In-flight performance of SilEye-2 experiment and cosmic ray abundances inside the Mir space station, *J. Phys. G*, 27, 2051-64 (2001)
- [3] M. Casolino, Bidoli V., Morselli A. et al, Dual origins of light flashes seen in space, *Nature*, 422, 680 (2003)
- [4] NASA, *Strategic Program Plan for Space Radiation Research*, NASA, Washington DC (1998). [http://spaceresearch.nasa.gov/docs/radiation\\_strat\\_plan\\_1998.pdf](http://spaceresearch.nasa.gov/docs/radiation_strat_plan_1998.pdf)
- [5] Reitz G., Beaujean R, Heilmann C et al., Dosimetry on the Spacelab missions IML1 and IML2, and D2 and on MIR, *Rad. Meas*, 26, 979-86 (1996)
- [6] Sakaguchi T. et al, LET distribution measurement with a new real-time radiation monitoring device-III onboard the Space Shuttle STS-84, *NIM A* 437, 75-87 (1999)
- [7] Badhwar G.D., Shurshakov V.A., Tsetlin V.V., Solar modulation of dose rate onboard the Mir station , *IEEE Trans. on Nuc. Science* 44(6), 2529-41 (1997)
- [8] Badhwar, G.D., Cucinotta, F. A., Depth Dependence of Absorbed Dose, Dose Equivalent and Linear Energy Transfer Spectra of Galactic and Trapped Particles in Polyethylene and Comparison with Calculations of Models , *Rad. Res.* 149, 209-18, 1998.
- [9] Yasuda H, Badhwar G.D., Komiyama T, Fujitaka K., Effective dose equivalent on the ninth Shuttle-Mir mission (STS-91), *Rad. Res.* 154(6), 705-13 (2000)
- [10] Beaujean R., Kopp J., Reitz G., Active dosimetry on recent space flights, *Rad Prot Dosim* 85(1-4 Pt2), 223-6 (1999)
- [11] Badhwar G.D., Radiation measurements on the ISS, *Phys. Medica* XVII, Suppl. 1, 287-91 (2001)
- [12] Reitz G.D., European dosimetry activities for the ISS, *Phys. Medica* XVII, Suppl. 1, 283-6 (2001)
- [13] Durante M., Radiation protection in space, *Riv. Nuovo Cimento*, 25, 8/1-8/70 (2002).
- [14] Durante M., Biological effects of cosmic radiation in low-Earth orbit, *Int. J. Mod. Phys A*, 17, 1713-21 (2001)
- [15] Durante M., Bonassi S., George K., Cucinotta F.A., Risk estimation based on chromosomal aberrations induced by radiation, *Radiat. Reas.* **156**, 662 (2001)
- [16] Casolino M., Bidoli V., Furano G. et al., The Sileye-3/Alteino experiment on board the ISS, *Nuc. Phys. B*, 113B, 71-8 (2002)
- [17] Bidoli V., Casolino M., De Pascale M.P. et al., The Sileye-3/Alteino Experiment for the Study of Light Flashes, Radiation Environment and Astronaut Brain Activity on Board the International Space Station, *J. Radiat. Res.*, 43, S47-S52 (2002)
- [18] Casolino M., et al, Detector Response and calibration of the cosmic ray detector of the Sileye-3/Alteino experiment, in press on *Adv. Spa. Res.*
- [19] Simpson J.A., *Ann. Rev. Nucl. Part. Phys.* 33, 323(1983)